Histochem Cell Biol (2006) 126: 57–69
DOI 10.1007/s00418-006-0146-9

ORIGINAL PAPER

Sven Saussez · Francois Lorfevre · Denis Nonclercq
Guy Laurent · Sabine André · Fabrice Journé
Robert Kiss · Gérard Toubeau · Hans-Joachim Gabius

Towards functional glycomics by localization of binding sites for tissue lectins: lectin histochemical reactivity for galectins during diethylstilbestrol-induced kidney tumorigenesis in male Syrian hamster

Accepted: 14 December 2005 / Published online: 25 January 2006

Abstract Endogenous lectins act as effectors of cellular activities such as growth regulation, migration, and adhesion. Following their immunohistochemical localization in our previous study (Saussez et al. in Histochem Cell Biol 123:29–41, 2005) we purified several galectins and used them as tools for monitoring accessible binding sites. Herein, we report the use of galectin histochemistry for the analysis of diethylstilbestrol (DES)-induced renal tumors in male Syrian hamster kidney (SHKT). Sections of normal kidney and DES-treated kidney were analyzed with biotinylated galectins-1, -3 (full-length and truncated), and -7. Accessible binding sites were detected, localization was predominantly extracellular and confined to medium-sized and large tumors. Monitoring the SHKT-derived HKT-1097 line, processed in vitro or as xenograft material, cytoplasmic and nuclear staining for galectins-1, -3, and -3tr could be observed. Adaptation of SHKT cells to long-term growth in culture is thus associated with emergence of this signal. Our data set illustrates the feasibility to complement immunohistochemical data by application of the tissue lectins as probes, and to detect regulation of galectin reactivity with differential characteristics within tumor progression in vivo and unique features of the tumor cell line in vitro and in vivo.

Keywords Diethylstilbestrol · Galectin · Lectin · Malignancy · Renal carcinogenesis

Abbreviations BC: Bowman's capsule · DES: Diethylstilbestrol · DMEM: Dulbecco's modified Eagle medium · DPBS: Dulbecco's PBS · ECM: Extracellular matrix · FBS: Fetal bovine serum · ISOM: Inner stripe of the outer medulla · LI: Labeling index · LT: Large tumor · MOD: Mean optical density · MT: Medium-sized tumor · NGS: Normal goat serum · OSOM: Outer stripe of the outer medulla · PAF: Paraformaldehyde · PAS: Periodic acid-Schiff · PTAV: Perivascular tissue surrounding arcuate artery and vein · RCC: Renal cell carcinoma · s.c.: Subcutaneous · SHKT: Syrian hamster kidney tumor · TB: Tumorous buds

S. Saussez (✉) · Francois Lorfevre · D. Nonclercq
G. Laurent · Gérard Toubeau
Laboratory of Histology, Faculty of Medicine and Pharmacy, University of Mons-Hainaut, Avenue du Champ de Mars, 6—Pentagone 1B, 7000 Mons, Belgium
E-mail: sven.saussez@umh.ac.be
Tel.: +32-65-373562
Fax: +32-65-373557

S. Saussez (✉) · Francois Lorfevre
Department of Anatomy, Faculty of Medicine and Pharmacy, University of Mons-Hainaut, Avenue du champ de Mars, 6—Pentagone 1B, 7000 Mons, Belgium

S. André · H.-J. Gabius
Institute of Physiological Chemistry, Faculty of Veterinary Medicine, Ludwig-Maximilians-University, Veterinärstr. 13, 80539 Munich, Germany

Fabrice Journé
Laboratory of Endocrinology/Bone Diseases and Department of Medicine, Institut Jules Bordet, Université Libre de Bruxelles, 1 Rue Héger-Bordet, 1000 Brussels, Belgium

R. Kiss
Laboratory of Toxicology, Institute of Pharmacy, Université Libre de Bruxelles, Campus Plaine CP 205/1, Blvd du Triomphe, 1050 Brussels, Belgium

Introduction

Malignant transformation is associated with changes in the cell phenotype. In addition to alterations in the proteomic profile the most frequent posttranslational modification, i.e. glycosylation, is also affected (Brockhausen et al. 1998; Hakomori 1998). Changes in the glycomic profile can readily be mapped by application of plant/invertebrate lectins (Caselitz 1987; Spicer and Schulte 1992), and the interpretation of the detected changes has initially focused on its phenotypic value. The concept of the sugar code, i.e. the realization that

carbohydrate epitopes store and transmit biological information, and the growing evidence for the presence of endogenous lectins have led to a paradigmatic shift of this original view (Gabius et al. 2004). In fact, tumor-associated remodeling of glycans will change a cell's display of signals and the interaction with endogenous lectins translates these signals into responses (Gabius 2001; Villalobo et al. 2006). Of special importance in this respect are the spatially accessible branch-end glycans, i.e. β-galactosides which are subject to frequent substitutions and hereby enable versatile signal generation. Case studies with galectin-1, a lectin homing in on terminal β-galactosides, have underscored the clinical relevance of its interaction with tumor cell glycans, because it triggers growth regulation in several tumor classes or tumor invasion in glioblastoma cells (Camby et al. 2002; Rappl et al. 2002; André et al. 2005a). As documented by structural analysis, an extended binding site is instrumental for enabling this lectin to be target selective (Siebert et al. 2003; López-Lucendo et al. 2004). Moreover, lectin reactivity is regulated by glycan substitutions or by modulating the density of glycan presentation (Unverzagt et al. 2002; André et al. 2004a; Wu et al. 2004). Thus, the concept of a functional link between altered glycosylation and cell responses involving endogenous lectins warrants study.

Due to the versatile functionality of galectins in growth/adhesion regulation, we have started the analysis of galectin-dependent parameters by immunohistochemically monitoring galectin expression in a tumor model (Saussez et al. 2005). Estrogen-induced renal tumors in adult male Syrian hamster (SHKT) represent an extensively used animal model for the study of hormonal and renal carcinogenesis, which can potentially provide insights to understanding origin and progression of related human malignancies (Li and Li 1984, 1990; Li et al. 2001; Liehr 1997, 2001; Liehr et al. 1986). Of note, immunohistochemical analysis of steroid hormone receptor expression in human renal cell carcinomas (RCC) has detected estrogen and progesterone receptors in a small number of cases (Di Silverio et al. 1997; Brown et al. 1998; Langner et al. 2004). Moreover, Orovan and Ryan (1989) have established that 16% of patients suffering from RCC are positive for estrogen receptor, albeit characterized by a low binding capacity. Also of relevance, a multicenter population-based case-control study intimated a correlation between hormonal and reproductive variables with risk of renal-cell cancer (Lindblad et al. 1995). Regarding therapeutic implications, combined chemoendocrine treatment with tegafur and tamoxifen showed slight benefit in advanced RCC (Wada et al. 1995). Previous work of our group (Toubeau et al. 2001; Nonclercq et al. 2002) has revealed that the distribution pattern of lineage markers in SHKT is intricate and evolves with the progression of diethylstilbestrol (DES)-induced neoplasms. Focusing on this model, we have detected marked intra-family differences in galectin expression when systematically studying tumor progression, galectins-1 and -3 already being present in preneoplastic cells and galectin-7 (p53-induced gene-1) only detectable in large tumors (LTs) (Saussez et al. 2005). The chimera-type galectin-3, which is monomeric in solution but undergoes aggregation in contact with multivalent cognate ligands (Ahmad et al. 2004), has already been defined as a developmentally regulated protein in baby hamster kidney cells, and its physiological relevance has highlighted its activity on cyst development or growth of the mouse ureteric tree (Foddy et al. 1990; Winyard et al. 1997; Bao and Hughes 1999; Bullock et al. 2001).

In the current study, we have taken our analysis of galectin-dependent parameters one step further by monitoring cell reactivity to galectins. The tissue lectins can specifically interact with a limited set of glycoconjugates and also with cytoplasmic and nuclear proteins such as Gemin4, the anti-apoptotic regulator bcl-2, the transcription factor TTF-1, β-catenin, and oncogenic H-Ras (Liu et al. 2002; Paron et al. 2003; Rotblat et al. 2004; Shimura et al. 2004; André et al. 2005b).

Thus, we have purified galectins-1, -3, and -7 and prepared biotinylated derivatives. To study the contribution of the collagenase-sensitive part of the chimera-type galectin-3 to glycan binding, we have prepared its truncated form. The questions that we address in this study are as follows: (1) Will the galectins localize accessible sites? (2) What is the pattern of galectin-reactive sites? (3) Are staining profiles similar or different? (4) Will tumor development alter galectin reactivity? (5) Will galectin reactivity be maintained in a stable cell line derived from the tumor model?

Materials and methods

Animals and treatment

Details of animal selection, housing, and treatment have been presented previously (Saussez et al. 2005). In brief, 11 groups of at least four animals were chronically treated with DES following a protocol similar to that previously reported in the literature for the same model (Nogueira et al. 1993). Implants containing 25 mg of DES (Sigma, St Louis, MO, USA) were inserted subcutaneously (s.c.) in the shoulder area of anesthetized animals and renewed every 2.5 months to maintain a constant blood level of DES. Hamsters were killed after 3, 8, 15 days, 1, 2, 4, 6, 7, 9, 10, and 11 months of DES exposure, respectively. A group of untreated animals ($n=8$) of various ages (3–9 months) was included as controls. Tissue specimens used in this study were deliberately selected to match samples examined by immunohistochemistry in the previous study (Saussez et al. 2005).

Preparation of biotinylated galectin derivatives

The different galectins produced by recombinant technology were purified by affinity chromatography on lactosylated Sepharose 4B prepared by divinyl sulfone

activation (Gabius 1990) as a decisive step, and were subjected to rigorous purity and activity controls by one- and two-dimensional gel electrophoresis, nano-electrospray ionization mass spectrometry, gel filtration, ultracentrifugation, hemagglutination, and solid-phase binding assays (André et al. 1999; Kopitz et al. 2003; Morris et al. 2004). The N-terminal section of the chimera-type galectin-3 was removed by collagenase D proteolysis to yield the C-terminal part of galectin-3 with the carbohydrate recognition domain, as described previously (Agrwal et al. 1993). After repurification of the truncated galectin-3, complete absence of the collagenase-sensitive sequence portion was ascertained by gel electrophoresis and gel filtration (André et al. 2004b). Biotinylation was carried out under activity-preserving conditions (Gabius et al. 1991), and the conjugates were rigorously controlled by solid-phase and cell-binding assays for the maintenance of carbohydrate-binding activity (André et al. 2004a). The extent of biotinylation was determined by a recently established proteomics approach (Purkrábková et al. 2003).

Galectin histochemistry

Tissue processing followed the protocol applied in our previous immunohistochemical study (Saussez et al. 2005). Briefly, kidney samples were fixed immediately after killing by immersion in Duboscq-Brazil fluid for at least 48 h and embedded in paraffin according to standard procedures. Sections of 4–5 μm thickness were cut serially with a Reichert Autocut 2040 microtome and mounted on silane-coated glass slides. Renal tissue samples and DES-induced renal tumors were then subjected to an optimized protocol to determine the presence of accessible binding sites, using the panel of biotinylated galectins, i.e. galectins-1, -3 (full-length or truncated versions), and -7.

Tissue sections were processed with biotinylated galectins following a slightly modified version of the standard streptavidin–biotin immunoperoxidase method (ABC method). The sensitivity of the method was increased by microwave pretreatment of dewaxed sections in 0.01 M citrate buffer (pH 6.0) for 2×5 min at 900 W. The sections were then preincubated in a solution containing 0.4% (v/v) hydrogen peroxide for 5 min to block endogenous peroxidase activity and thoroughly rinsed in phosphate-buffered saline (PBS; 0.04 M Na_2HPO_4, 0.01 M KH_2PO_4, and 0.12 M NaCl, pH 7.4). Thereafter, they were successively treated with avidin (0.1 mg/ml in PBS, 20 min) and biotin (0.1 mg/ml in PBS, 20 min) solutions to block false-positive signals due to the reactivity of endogenous biotin. After rinsing in PBS, the sections were incubated in 0.5% casein in PBS for 20 min and exposed sequentially at room temperature to the following reagents: (1) biotinylated galectins at the following dilutions defined by titration studies in each case: galectin-1 at 1/2,500, galectin-3 at 1/400, truncated galectin-3 at 1/400, and galectin-7 at 1/500 for 1 h; (2) ABC complexes for 30 min. Specifically bound peroxidase activity was visualized by incubation with solution containing the chromogenic substrate (0.02% 3,3′-diaminobenzidine–0.01% H_2O_2 in PBS). After each step of the staining procedure the sections were rinsed in PBS to completely remove unbound reagents. The sections were finally counterstained with PAS, hemalun, and luxol fast blue and mounted in a permanent medium. Controls for the specificity of galectin-dependent labeling included the omission of the incubation step with labeled lectin from the processing to assess probe-independent staining. Moreover, lactose/asialofetuin inhibition as routinely applied in histochemical glycan profiling by lectins was included to block β-galactoside-specific binding and protein-epitope-dependent binding sensitive to lactose (Manning et al. 2004).

Grading of DES-induced renal tumors

Neoplasms were graded according to size and gross morphology as detailed previously (Saussez et al. 2005). Briefly, three stages were defined on the basis of the following criteria: (1) tumorous buds (TB): well-defined, small clusters of tumor cells surrounded by normal kidney tissue (5–200 cells covering a section area of 350 to approx. 15,000 μm^2); (2) medium-sized tumors (MT): clusters of increased size with tumor cells infiltrating normal kidney tissue (area > 15,000 μm^2, up to 300,000 μm^2; approx. diameter of 150–600 μm); (3) LT: invasive tumors of large diameter extensively infiltrating the kidney (> 300,000 μm^2 and up to 80 mm^2).

Computer-assisted morphometry

The staining profiles of the sections that were processed for galectin histochemistry were quantitatively characterized by using the software KS 400 imaging system (Carl Zeiss vision, Hallbergmoos, Germany). As is common practice, the labeling index (LI) is defined as the percentage of neoplastic tissue area specifically stained by a given probe, while the mean optical density (MOD) denotes the mean staining intensity of the malignant cells. This method of computer-assisted quantification has been rigorously standardized and described in detail (Nagy et al. 2002, 2003).

Cell culture and fluorescence cytochemistry

The HKT-1097 cell line (DSMZ no. ACC 445) was derived from kidney tumors induced in male Syrian golden hamsters by prolonged exposure to DES for a period of 11 months (Laurent et al. 1999). Cell culture was performed at 37°C in a cell incubator with humidified atmosphere at 5% CO_2. For routine propagation, cells were grown in 75-cm^2 flasks containing Dulbecco's modified Eagle Medium (DMEM, Cambrex Bioscience,

Verviers, Belgium) supplemented with 10% fetal bovine serum (FBS) (HyClone, Logan, UT, USA), 25 mM *N*-2-hydroxyethylpiperazine-*N*′-2-ethanesulfonic acid, 2 mM L-glutamine, 100 U/ml penicillin G, 100 μg/ml streptomycin, and 0.25 μg/ml amphotericin B (Invitrogen/Gibco, Merelbeke, Belgium). Cells were passaged once a week, with complete renewal of the culture medium every 2 days after seeding. For subculture, the cell monolayers were rinsed with Dulbecco's PBS (DPBS) and detached from the plastic surface by treatment with trypsin/EDTA solution. Cell numbers in suspensions were determined in a model Z1 electronic cell counter (Beckman Coulter, Fullerton, CA, USA).

For fluorescence studies, HKT-1097 cells were plated at a density of 5,000 cells/cm^2 on sterile round glass coverslips in 12-well dishes. Two days after seeding, the cell monolayers were carefully rinsed with DPBS and fixed for 15 min with ice-cold 4% paraformaldehyde (PAF) in the same buffer. After fixation, PAF was changed for DPBS wherein the cells were kept at 4°C prior to processing for staining which was performed routinely within the next 20 h.

Cell cultures were processed for fluorescence cytochemistry according to a modified procedure previously described for immunofluorescence staining of these cells (Laurent et al. 1999). Cell monolayers were rinsed several times with PBS containing 0.1% Triton X-100. Prior to incubation with a solution containing a biotinylated galectin, cells were preincubated for 20 min in PBS containing 5% normal goat serum (PBS-NGS) and 0.05 M NH_4Cl to prevent nonspecific adsorption of proteins. Cells were exposed for 60 min to solutions containing biotinylated galectins at a 1/50 dilution in PBS-NGS. Labeling was completed by incubating cells for 30 min with a solution containing Texas Red-labeled streptavidin (Vector Laboratories, Burlingame, CA, USA). After final rinses in PBS, the coverslips were mounted on glass slides using commercial anti-fading medium (Vectashield®, Vector Laboratories). Negative controls were run by omitting the incubation step with the biotinylated probe in order to exclude probe-independent binding.

The cell preparations were analyzed by fluorescence microscopy as indicated above. Excitation wavelength of 596 nm and emission wavelength of 615 nm were used for monitoring of Texas Red fluorescence. The staining profile of processed cell preparations was documented by using a PC-driven digital camera (Leica DC 300F, Leica Microsystems AG, Heerbrugg, Switzerland). Microscopic fields were digitalized by a software specifically designed for image acquisition and storage (Leica IM 50). Image adjustment and printing used appropriate softwares (Corel PHOTO-PAINT ™ and CorelDRAW ™, Corel Corporation, Ottawa, Canada).

Quantitative analysis of the intracellular distribution of fluorescence signal was performed on digitalized images using Image J (a public domain image analysis software developed by W. Rasband at the Research Services Branch of the National Institute of Mental Health, NIH). Images were analyzed in the red channel after RGB split. For each cell, mean gray level was first determined for the whole cell surface (whole cell signal), followed by the determination of mean gray level in the nuclear area (nuclear signal). Signal distribution between nucleus and cytoplasm was then assessed by calculating the nuclear/whole cell signal ratio. Values given for each biotinylated galectin are means (± SD) of more than ten determinations.

HKT-1097 in vivo tumorigenicity

HKT-1097 cell tumorigenicity in male nude mice (Swiss strain) (Iffa Credo, Brussels, Belgium) was exploited to obtain tumor xenografts for galectin histochemistry on material of the cell line grown in vivo. HKT-1097 cells were plated at an initial density of 10^4 cells/cm^2 in 75-cm^2 flasks. Three days after seeding, cells were harvested by trypsinization, the cell-containing suspension was centrifuged and the cells were resuspended in serum-free DMEM without Phenol Red. Cell concentration in suspensions was adjusted to 5×10^7 cells/ml. Two hundred-microliter aliquots of the cell suspension (s.c. injection into the left flank) were injected per animal. Development of tumor xenograft was monitored weekly. Xenografts were finally obtained at necropsy, fixed in Duboscq-Brazil fluid and processed as described above for galectin histochemistry.

Results

The first step of our study consisted in labeling the endogenous lectins without impairing their carbohydrate-binding activity using the *N*-hydroxysuccinimide ester derivative of biotin. As monitored by a recently developed proteomics protocol, the p*I* values of the galectins were shifted as a result of amino group substitution involved in biotin incorporation, thereby allowing calculation of the number of added biotin molecules (Purkrábková et al. 2003). This procedure resulted in measuring incorporation yields of 8–11 label units for galectin-1, 4–9 for galectin-3, and 2–5 for galectin-7, independently controlled by standard titration analysis using avidin. Solid-phase assays in microtiter plate wells using the surface-immobilized glycoprotein asialofetuin as ligand—a situation resembling lectin binding to the sections' surface—as certained maintenance of carbohydrate-binding activity. Thus, these galectins could be introduced for monitoring the expression of binding sites on the panel of tissue specimen which had been processed previously for the immunohistochemical detection of galectins (Saussez et al. 2005).

We first analyzed the reactivity of sections of normal hamster kidneys. Binding of the labeled galectins was detected and it was present in different parts of the tissue sections as summarized in Table 1 for normal renal tissue. Upon galectin histochemical staining, distinct structural elements were positive in the normal kidney,

Table 1 Staining profile of tumors by tested biotinylated galectins

Biotinylated probes	Distribution profile of staining
Galectin-1	BC, PTAV, OSOM
Galectin-3 (full-length)	BC, PTAV, OSOM, ISOM
Galectin-3 (truncated)	BC, PTAV, OSOM, ISOM
Galectin-7	BC, PTAV, OSOM, ISOM

Abbreviations for the different areas in the kidney followed standard nomenclature for renal structures (Kriz and Bankir 1988): *BC* Bowman's capsule, *PTAV* perivascular tissue surrounding arcuate artery and vein, *OSOM* outer stripe of the outer medulla, *ISOM* inner stripe of the outer medulla

i.e. Bowman's capsule, perivascular tissue around arcuate artery and vein, extracellular matrix (ECM) of the outer stripe of the outer medulla (surrounding proximal straight tubules), and the ECM of the inner stripe of the outer medulla (except for biotinylated galectin-1) (Fig. 1a, c, e). Staining was clearly sensitive to the presence of a mixture of the haptenic inhibitor lactose (0.1 M) and the galectin-binding glycoprotein asialofetuin (0.5 mg/ml) indicating interaction with ligands via the carbohydrate recognition domain. Regarding the chimera-type galectin the staining profile was not altered for the truncated probe without the collagenase-sensitive part. After having revealed that the biotinylated galectins can serve as histochemical tools in normal renal tissue and determined the individual staining profiles, we next addressed the issue as to whether malignant transformation may affect the staining profile.

The tumor incidence and progression in the DES-treated animals followed the previously described pattern (Wattiez et al. 1996; Nonclercq et al. 1998; Toubeau et al. 2001). The first cases of kidney neoplasms monitored by S100 protein expression appeared after 4–5 months of DES exposure. The MTs were observed

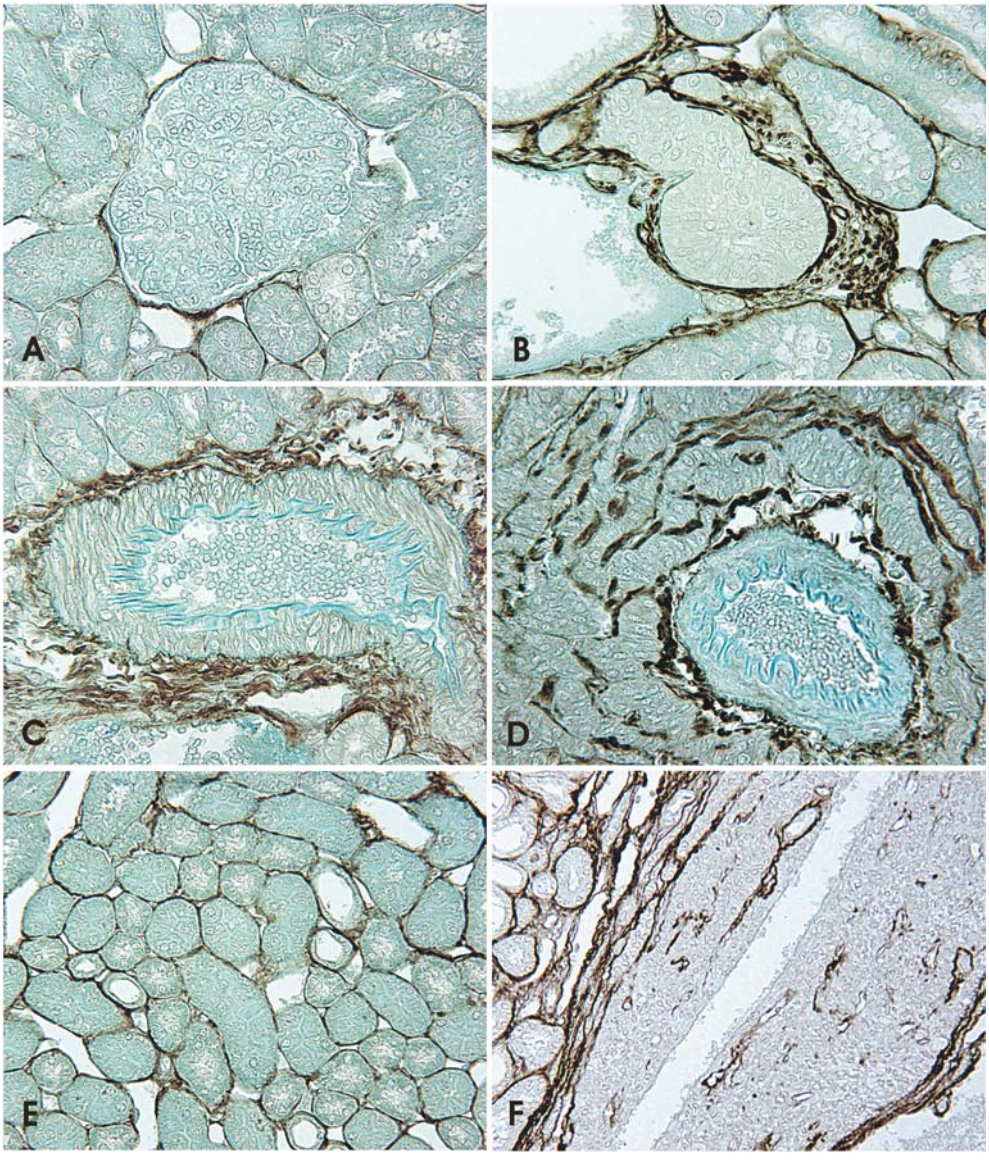

Fig. 1 Localization of binding sites for the truncated version of biotinylated galectin-3 in normal renal tissue (**a**, **c**, **e**) and in DES-induced renal tumors (**b**, **d**, **e**). Galectin reactivity was detected in the Bowman's capsule (**a**), perivascular tissue around arcuate artery and vein (**c**), extracellular matrix of the outer stripe of the outer medulla (surrounding proximal straight tubules) (**e**). Galectin reactivity was localized in the ECM of the peritumoral area after 7 months (**b**), 9 months (**d**), or 11 months (**f**) of DES exposure, respectively. Magnification **a**, **c**–**f** 100×, **b** 650×

after 6 months of DES exposure and LTs were encountered after 9 months of treatment. As noted for normal tissue, tumor tissue sections presented specific and spatially distinct staining (Fig. 1b, d, f). Using these data including those of the quantitative analysis and the previously presented evidence on galectin expression (Saussez et al. 2005), the course of changes in staining parameters during tumor development could be plotted (Fig. 2). As reported previously (Saussez et al. 2005), galectins-1 and -3 appeared at a very early stage during neoplastic transformation, small clusters of positive cells being already present after 1 month of DES exposure. Within these small clusters of preneoplastic cells, no galectin-binding sites were revealed using biotinylated galectins-1, -3, -3tr, and -7. In the course of tumor progression, staining was seen in the peritumoral area of MTs in the vicinity of fusiform cells of the interstitial tissue, decorating the ECM (Fig. 1b, d, f). This staining was similar for the biotinylated galectins-1, -3, -3tr, and -7. No cytoplasmic or nuclear labeling was observed. In LTs, galectin-reactive sites were observed in the peritumoral area and also in the interstitial septa within the tumoral mass (Fig. 1d, f). Herewith, we have answered the first two questions given at the end of Introduction.

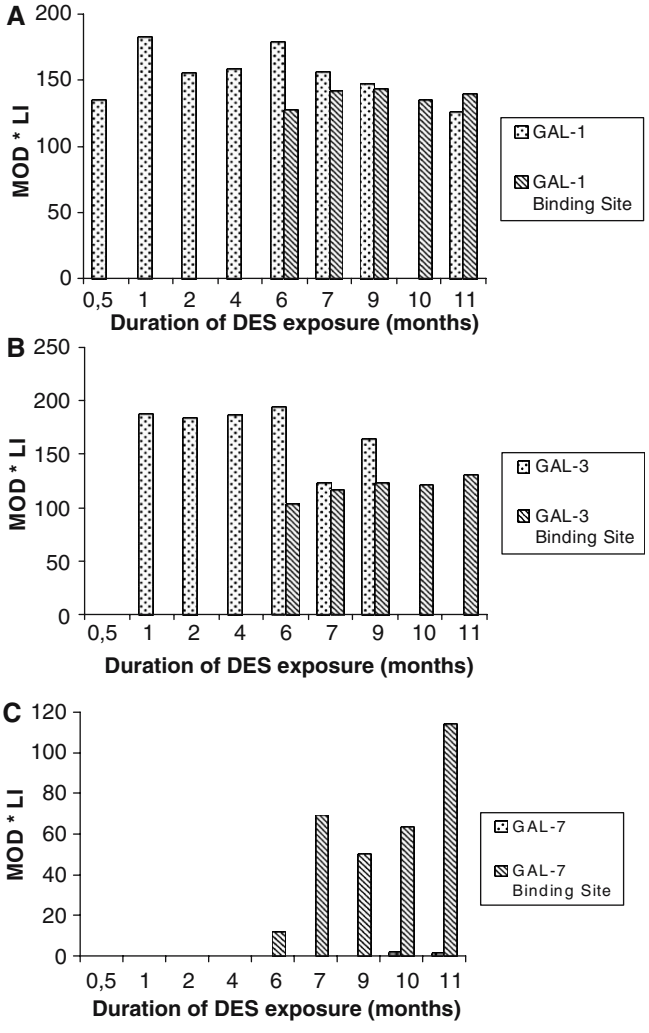

Fig. 2 Comparison of the changes in staining profiles of galectin-1 (**a**), galectin-3 (**b**), and galectin-7 (**c**) as reported previously (Saussez et al. 2005) and of the localization of accessible binding sites for each galectin

In order to determine whether the staining profiles with the individual probes are similar or different, we next analyzed serial sections of tumors after different lengths of DES exposure. Expression of the S100 protein as a specific marker of tumor tissue was used as an internal control (Toubeau et al. 2001). Quantitative assessment revealed strong positivity for MOD in the case of galectin-7 (Table 2). Staining profiles using biotinylated galectins-1 and -3 (full-length and truncated proteins) can be either very similar or different. Figure 3 illustrates that the positive staining present in the peritumoral area of a LT is sometimes close for those probes (Fig. 3b–d) but can also be different (Fig. 3f–h). Removal of the collagenous stalk of galectin-3 reduced the LI of LTs conspicuously (Table 2). The homodimeric galectins-1 and -7 thus react differently, and staining properties of LTs are sensitive to the presence of the N-terminal section of galectin-3. Tumor progression is not associated with major alterations in extent of accessibility of sites with reactivity to galectins, herewith only leaving the last question of Introduction unaddressed.

Table 2 Quantitative aspects of galectin-dependent staining of SHKT

	Duration of DES exposure (months)				
	6	7	9	10	11
Gal-1					
Medium-sized tumor					
MOD	129	145			
LI	98	98			
Large tumor					
MOD			145	136	141
LI			99	99	99
Gal-3					
Medium-sized tumor					
MOD	115	118			
LI	89	98			
Large tumor					
MOD			125	124	133
LI			99	98	98
Gal-3tr					
Medium-sized tumor					
MOD	136	150			
LI	84	93			
Large tumor					
MOD			138	128	141
LI			36	53	76
Gal-7					
Medium-sized tumor					
MOD	162	158			
LI	7	44			
Large tumor					
MOD			142	135	143
LI			35	47	80

MOD mean optical density (values ranging from 0 to 255), *LI* labeling index (in percent)

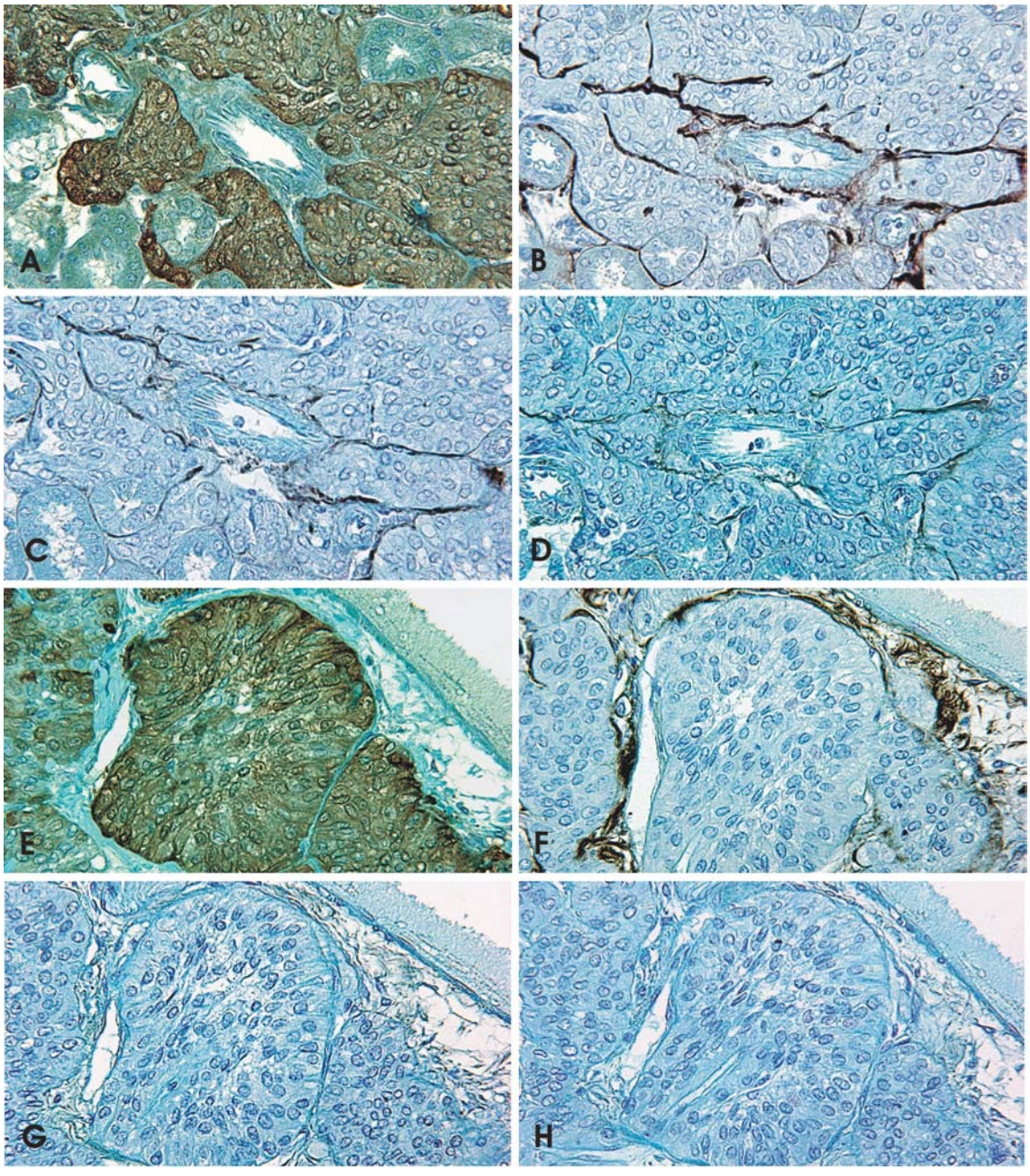

Fig. 3 The staining profiles for sites reactive with galectin-1, galectin-3, and galectin-3tr are compared in serial sections of large tumors from animals exposed to DES for 9 (**a**–**d**) or 10 months (**e**–**h**), respectively. In **a**, S100 protein has been used as marker of tumor tissue. **b**–**d** Galectin-1, truncated version of galectin-3 and galectin-3 histochemistry. Staining can be observed in the peritumoral area of large tumor and the patterns exhibit obvious similarity. **e** Large tumor positive for S100 protein. **f**–**h** Pattern of sites reactive with labeled galectin-1 (**f**), the truncated version of galectin-3 (**g**), and full-length galectin-3 (**h**). Magnification **a**–**h** 650×

In order to answer this question, the HKT-1097 cell line derived from renal tumors (Laurent et al. 1999) was processed by fluorescence cytochemistry using biotinylated galectins. In principle, HKT-1097 cells were found to be reactive with the galectins, as seen for sections of SHKT. Differences were noted when comparing the intracellular distribution profiles of the fluorescence signal. Biotinylated galectin-1 produced a strong nuclear signal (Fig. 4a, nuclear/whole cell signal ratio 1.89 ± 0.25) whereas fluorescence staining was weaker and more evenly distributed for truncated biotinylated galectin-3 (Fig. 4e, nuclear/whole cell signal ratio 1.61 ± 0.14) and in particular for full-length galectin-3 (Fig. 4c, nuclear/whole cell signal ratio 1.41 ± 0.07; Table 3). Fluorescence staining was frequently seen in the perinuclear area and exhibited a reticular appearance suggestive of an association of binding site with intracellular membranes. When cells were xenotransplanted

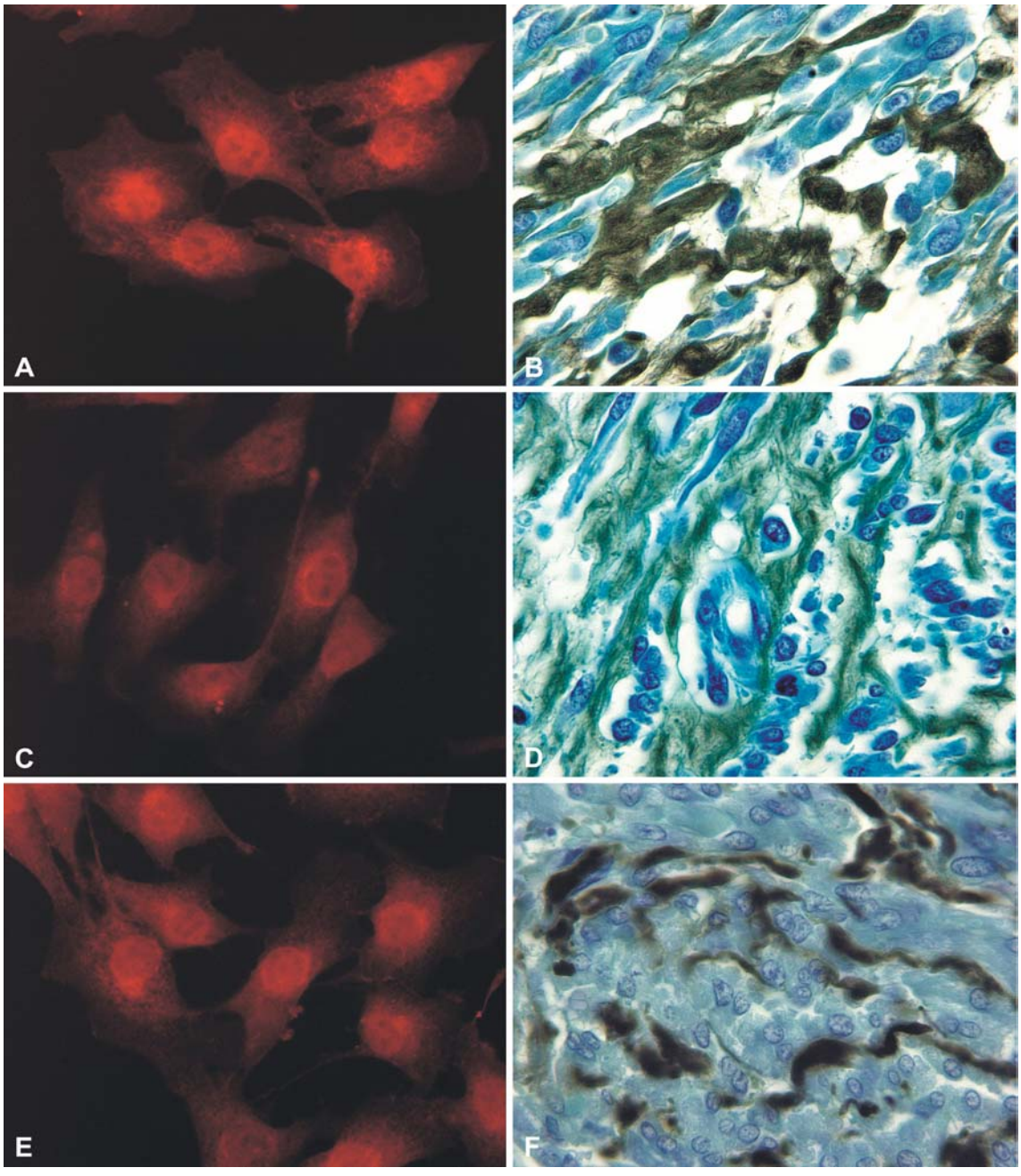

Fig. 4 Fluorescent detection of biotinylated galectins in cells of the HKT-1097 line (**a**, **c**, **e**). Lectin reactivity was detected using biotinylated galectin-1 (**a**), full-length galectin-3 (**c**), or its truncated version (**e**). Texas Red labeling. Magnification **a**, **c**, **e** 650×. Histochemical localization of biotinylated galectin-1 (**b**), galectin-3 (**d**), and the truncated version of galectin-3 in sections of tumors obtained from nude mice after implantation of cells of the HKT-1097 line. Magnification **b**, **d**, **f** 845×

and tumor xenografts were recovered after the s.c. implantation of HKT-1097 cells, the comparison between sections of these tumors and sections of primary SHKT revealed marked differences. Whereas neither nuclear nor cytoplasmic staining had been observed during tumor progression in the SHKT model, processing with biotinylated galectin-1 resulted in a strong nuclear and cytoplasmic staining in a small number of cells (Fig. 4b; Table 3). The ECM was also intensely stained. Moreover, removal of the collagenase-sensitive N-terminal part of galectin-3 produced a clear difference in staining pattern (Fig. 4f). Using this truncated version of biotinylated galectin-3, we observed strong labeling of the ECM as well as nuclear and cytoplasmic labeling in a small subpopulation of cells (Fig. 4f; Table 3). By contrast, treatment with full-length galectin-3 (Fig. 4d) and galectin-7 only resulted in a weak signal in the ECM. Again, a difference in staining between the proto-type

Table 3 Distribution of galectin-dependent staining in SHKT

	Extracellular matrix		Cytoplasm		Nucleus		Cell membrane
In vivo							
Medium tumors	+ +	Gal-1					
	+	Gal-3					
	+ + +	Gal-3tr					
	+ + +	Gal-7					
Large tumors	+ + +	Gal-1					
	+ +	Gal-3					
	+ +	Gal-3tr					
	+ + +	Gal-7					
Xenograft							
HKT 1097 in nude mice	+ + +	Gal-1	+ + +	Gal-1	+ + +	Gal-1	
	+	Gal-3	+ + +	Gal-3	+ + +	Gal-3	
	+ + +	Gal-3tr	+ + +	Gal-3tr	+ + +	Gal-3tr	
	+	Gal-7	+ + +	Gal-7	+ + +	Gal-7	

galectins-1 and -7 is thus noted. Using a mixture of lactose/asialofetuin to block β-galactoside-specific binding, we observed a clear-cut decrease of the cellular staining (Fig. 5a, b) and a complete disappearance of the staining of the ECM (Fig. 5c, d). This sensitivity to presence of lactose/asialofetuin was similar for all used probes.

Discussion

The study of cellular effectors includes two main steps: (a) the detection of effector presence and (b) the analysis of reactants. Previous work of our group has demonstrated by immunohistochemistry the expression of

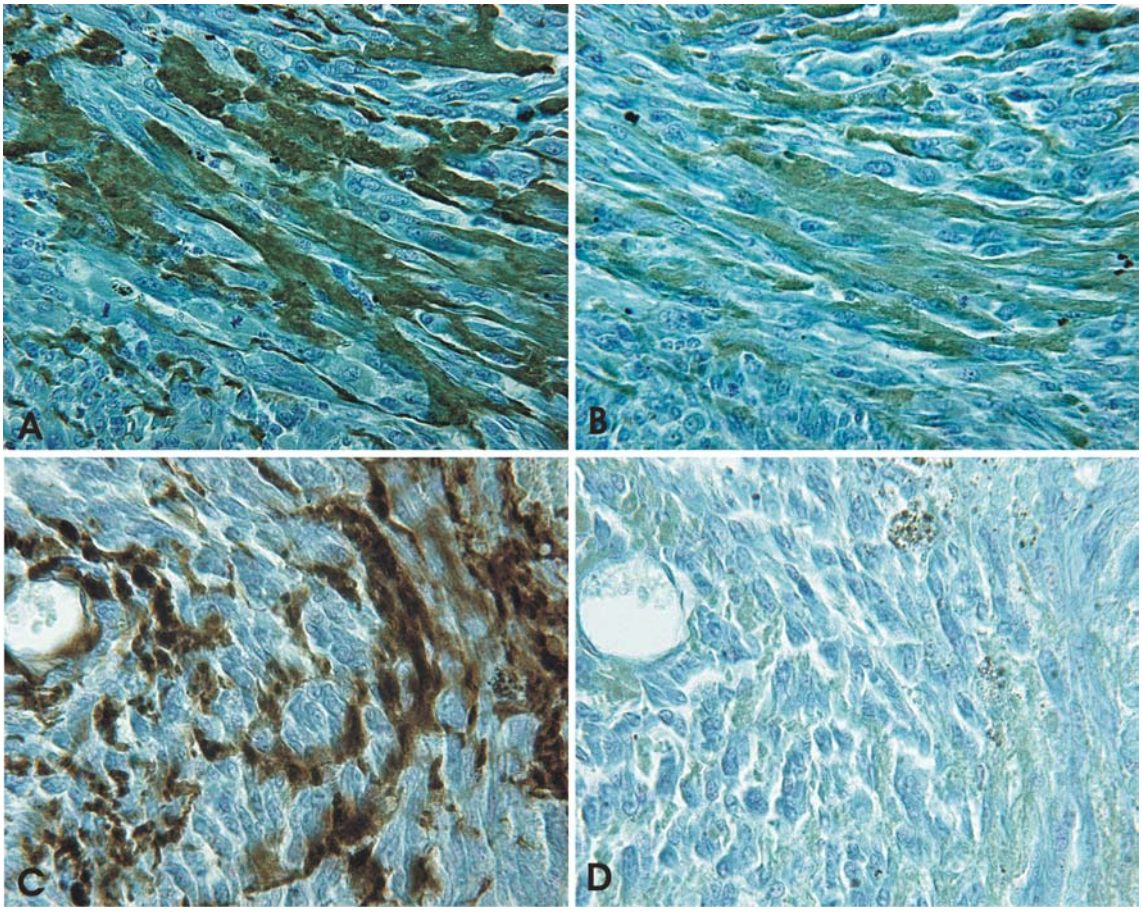

Fig. 5 Control for carbohydrate-dependent inhibition of binding using biotinylated galectin-1 (**a**, **b**) and truncated galectin-3 (**c**, **d**) in the absence (**a**, **c**) or the presence (**b**, **d**) of a mixture of lactose and the glycoprotein asialofetuin on sections of tumors obtained from nude mice after implantation of cells of the HKT-1097 line. Magnification **a**–**d** 650×

adhesion/growth-regulatory galectins in a model of estrogen-induced renal tumorigenesis (Saussez et al. 2005). In the current study, we used biotinylated galectins as a tool to explore by histochemistry the occurrence and distribution of reactive sites during the course of tumor development. Taken together, present data and our previously published immunohistochemical observations provide insights into the two sides of this molecular system involving the adhesion/growth-regulatory galectins. By systematic quantitative monitoring we could thus answer the questions listed at the end of Introduction.

The use of different biotinylated galectins enabled us to detect accessibility of binding sites and monitor their spatial and temporal patterns of localization. During the first 6 months of DES exposure, we did not observe any sites accessible to the probes in the cortico-medullary junction. Galectins-1 and -3 but not -7 were detected in small, putative preneoplastic lesions (Saussez et al. 2005). It is thus likely that galectins occupy functional sites at this stage completely. The lack of extracellular staining is an indication for the target specificity of the mammalian probe. A connection between steroid hormones and a galectin has been drawn previously physiologically. Regulation of galectin-1 expression by a steroid hormone has been documented during implantation, where its expression in mouse uterus is under the control of ovarian steroids (Choe et al. 1997). In this case, uterine mRNA specific for galectin-1 was up-regulated 6 h after 17β-estradiol injection and blocked by the estrogen receptor antagonist ICI182780. Because the reproductive and urogenital tracts in the Syrian hamster arise from the same embryonic germinal ridge, it can be assumed that the kidney retains estrogen sensitivity. A putative steroid hormone receptor binding site with only three nucleotide changes from the consensus sequence is located in the upstream region of the human galectin-1 gene at position −210 (Gitt and Barondes 1991). Steroid responsiveness is also seen for glucocorticoids in the human T cell leukemia line CEM C7 and clinical material of nasal polyps (Goldstone and Lavin 1991; Delbrouck et al. 2002). Studies on galectin-1 expression in postnatal development of rat lung have indicated that translation and degradation are further levels of regulation by dexamethasone (Clerch et al. 1987; Sanford et al. 1993). Thus, galectin-1 expression observed in the preneoplastic clusters might be attributed to DES exposure.

Concomitantly with the progression to MT, galectin reactivity was detected in the ECM of the peritumoral area. Immunoreactivities for galectins-1 and -3 have been previously detected in fusiform cells in this compartment (Saussez et al. 2005). Several reports support the view that a subset of germinal stem cells are prone to genomic instability when exposed to estrogen treatment (Hou et al. 1996; Li et al. 1999). After 5 and 6 months of continuous estrogen treatment, the expression of the early estrogen-response genes—in particular, c-*myc* and c-*fos*—rose significantly in estrogen-induced renal tumors (Bhat et al. 1995; Hou et al. 1996), and chromosome 6 where c-myc is localized exhibited a high frequency of trisomies and tetrasomies in the kidney and in primary renal tumors (Li et al. 1999). These data suggest that the detected estrogen-induced genomic instability after 5 months of treatment may be a key step in the carcinogenic process. This minimal duration of DES exposure to observe genomic instability relates to the period to detect accessible sites for galectins.

Evidently, tumor progression is associated with increased availability of accessible sites, matching the presence of the lectins. Large tumors presented binding sites for galectins used as probes in the interstitial septa and in the peritumoral area without any nuclear or cytoplasmic staining in tumor cells. Serial sections of LTs indicated a tendency for heterogeneity of the staining patterns. To assess the cellular stability of galectin reactivity, we extended the histochemical analysis of galectin-binding sites to the HKT-1097 cell line derived from SHKT. In addition, tumor xenografts recovered after HKT-1097 s.c. implantation in nude mice were also processed. Fluorescence staining of cultured cells disclosed a different distribution of galectin-binding sites, compared with that observed in primary SHKT. In fact, these binding sites were present intracellularly in HKT-1097 cells. Nuclear and cytoplasmic signals remained intense and stable when studying sections of xenograft tumors. Thus, the presence of nuclear galectin-binding sites appears to be linked to advanced stage of tumor progression, because this feature is only observed in a stable tumor-derived cell line and in tumor xenograft tissue. This finding is consistent with the results of a study relating galectins-1 and -3 reactivities to unfavorable prognosis for patients with grade II and III RCC (Francois et al. 1999). Moreover, gene array analysis in RCCs has established that galectins-1 and -3 were overexpressed, pointing to their potential as diagnostic markers (Young et al. 2001).

In conclusion, we have extended our previous immunohistochemical study by assessing galectin reactivities. Herein, we analyzed the spatial and temporal localization patterns of specific binding sites with galectin-type specificity in an experimental model of carcinogenesis. We answer the issues raised in Introduction by showing that: (1) galectin probes reveal a distinct profile of staining, (2) galectin-binding sites are primarily localized in the ECM surrounding medium-sized and LTs, (3) differences in staining properties are apparent between the homodimeric galectins-1 and -7 and also an influence of the N-terminal domain of galectin-3 was noted, (4) small-sized versus medium-sized and large tumors differ in their reactivities for galectins, and (5) the cell line and xenografts acquire nuclear and cytoplasmic sites, suggesting that an intracellular localization of galectin-binding sites could be correlated to advanced stage of tumor progression.

Acknowledgements R. Kiss and G. Laurent are Research Director and Senior Research Associate, respectively, of the National Fund for Scientific Research (Belgium). G. Laurent is the recipient of a grant (no. 3.4512.03) from the Belgian Fund for Medical Scientific Research and H.-J. Gabius of grants from the Mizutani Foundation for Glycoscience (Tokyo, Japan) and the Verein zur Förderung des biologisch-technologischen Fortschritts in der Medizin e.V. (Heidelberg, Germany). The expert technical assistance of G. Ninfa is gratefully acknowledged.

References

Agrwal N, Sun Q, Wang SY, Wang JL (1993) Carbohydrate-binding protein 35. I. Properties of the recombinant polypeptide and the individuality of the domains. J Biol Chem 268:14932–14939

Ahmad N, Gabius HJ, André S, Kaltner H, Sabesan S, Roy R, Liu B, Macaluso F, Brewer CF (2004) Galectin-3 precipitates as a pentamer with synthetic multivalent carbohydrates and forms heterogeneous cross-linked complexes. J Biol Chem 279:10841–10847

André S, Kojima S, Yamazaki N, Fink C, Kaltner H, Kayser K, Gabius HJ (1999) Galectins-1 and -3 and their ligands in tumor biology. J Cancer Res Clin Oncol 125:461–474

André S, Unverzagt C, Kojima S, Frank M, Seifert J, Fink C, Kayser K, von der Lieth CW, Gabius HJ (2004a) Determination of modulation of ligand properties of synthetic complex-type biantennary N-glycans by introduction of bisecting GlcNAc *in silico, in vitro* and *in vivo*. Eur J Biochem 271:118–134

André S, Kaltner H, Furuike T, Nishimura SI, Gabius HJ (2004b) Persubstituted cyclodextrin-based glycoclusters as inhibitors of protein–carbohydrate recognition using purified plant and mammalian lectins and wild-type and lectin-gene-transfected tumor cells as targets. Bioconjug Chem 15:87–98

André S, Kaltner H, Lensch M, Russwurm R, Siebert HC, Fallsehr C, Tajkhorshid E, Heck AJR, von Knebel Doeberitz M, Gabius HJ, Kopitz J (2005a) Determination of structural and functional overlap/divergence of five proto-type galectins by analysis of the growth-regulatory interaction with ganglioside GM_1 *in silico* and *in vitro* on human neuroblastoma cells. Int J Cancer 114:46–57

André S, Arnusch CJ, Kuwabara I, Russwurm R, Kaltner H, Gabius HJ, Pieters RJ (2005b) Identification of peptide ligands for malignancy- and growth-regulating galectins using random phage-display and designed combinatorial peptide libraries. Bioorg Med Chem 13:563–573

Bao Q, Hughes RC (1999) Galectin-3 and polarized growth within collagen gels of wild-type and ricin-resistant MDCK renal epithelial cells. Glycobiology 9:489–495

Bhat HK, Hacker HJ, Bannasch B, Thompson EA, Liehr JG (1995) Differential regulation by estrogen of c-fos in hamster kidney and estrogen-induced kidney tumor. Int J Oncol 7:527–534

Brockhausen I, Schutzbach J, Kuhns W (1998) Glycoproteins and their relationship to human disease. Acta Anat (Basel) 161:36–78

Brown DF, Dababo MA, Hladik CL, Eagan KP, White CL III, Rushing EJ (1998) Hormone receptor immunoreactivity in hemangioblastomas and clear cell renal cell carcinomas. Mod Pathol 11:55–59

Bullock SL, Johnson TM, Bao Q, Hughes RC, Winyard PJ, Woolf AS (2001) Galectin-3 modulates ureteric bud branching in organ culture of the developing mouse kidney. J Am Soc Nephrol 12:515–523

Camby I, Belot N, Lefranc F, Sadeghi N, de Launoit Y, Kaltner H, Musette S, Darro F, Danguy A, Salmon I, Gabius HJ, Kiss R (2002) Galectin-1 modulates human glioblastoma cell migration into the brain through modifications to the actin cytoskeleton and levels of expression of small GTPases. J Neuropathol Exp Neurol 61:585–596

Caselitz J (1987) Lectins and blood group substances as "tumor markers". Curr Top Pathol 77:245–277

Choe YS, Shim C, Choi D, Sang Lee C, Lee KK, Kim K (1997) Expression of galectin-1 mRNA in the mouse uterus is under the control of ovarian steroids during blastocyst implantation. Mol Reprod Dev 48:261–266

Clerch LB, Whitney PL, Massaro D (1987) Rat lung lectin synthesis, degradation and activation. Developmental regulation and modulation by dexamethasone. Biochem J 245:683–690

Delbrouck C, Doyen I, Belot N, Decaestecker C, Ghanooni R, de Lavareille A, Kaltner H, Choufani G, Danguy A, Vandenhoven G, Gabius HJ, Hassid S, Kiss R (2002) Galectin-1 is overexpressed in nasal polyps under budesonide and inhibits eosinophil migration. Lab Invest 82:147–158

Di Silverio F, Sciarra A, Flammia GP, Mariani M, De Vico A (1997) Multiple primary tumors: 17 cases of renal-cell carcinoma associated with primary tumors involving different steroid-hormone target tissues. World J Urol 15:203–209

Foddy L, Stamatoglou SC, Hughes RC (1990) An endogenous carbohydrate-binding protein of baby hamster kidney (BHK21 C13) cells. Temporal changes in cellular expression in the developing kidney. J Cell Sci 97:139–148

Francois C, van Velthoven R, De Lathouwer O, Moreno C, Peltier A, Kaltner H, Salmon I, Gabius HJ, Danguy A, Decaestecker C, Kiss R (1999) Galectin-1 and galectin-3 binding pattern expression in renal cell carcinomas. Am J Clin Pathol 112:194–203

Gabius HJ (1990) Influence of type of linkage and spacer on the interaction of β-galactoside-binding proteins with immobilized affinity ligands. Anal Biochem 189:91–94

Gabius HJ (2001) Glycohistochemistry: the why and how of detection and localization of endogenous lectins. Anat Histol Embryol 30:3–31

Gabius HJ, Wosgien B, Hendrys M, Bardosi A (1991) Lectin localization in human nerve by biochemically defined lectin-binding glycoproteins, neoglycoprotein and lectin-specific antibody. Histochemistry 95:269–277

Gabius HJ, Siebert HC, André S, Jiménez-Barbero J, Rüdiger H (2004) Chemical biology of the sugar code. ChemBioChem 5:740–764

Gitt MA, Barondes SH (1991) Genomic sequence and organization of two members of a human lectin gene family. Biochemistry 30:82–89

Goldstone SD, Lavin MF (1991) Isolation of a cDNA clone, encoding a human β-galactoside binding protein, overexpressed during glucocorticoid-induced cell death. Biochem Biophys Res Commun 178:746–750

Hakomori S (1998) Cancer-associated glycosphingolipid antigens: their structure, organization, and function. Acta Anat (Basel) 161:79–90

Hou X, Li JJ, Chen W, Li SA (1996) Estrogen-induced proto-oncogene and suppressor gene expression in the hamster kidney: significance for estrogen carcinogenesis. Cancer Res 56:2616–2620

Kopitz J, André S, von Reitzenstein C, Versluis K, Kaltner H, Pieters RJ, Wasano K, Kuwabara I, Liu FT, Cantz M, Heck AJR, Gabius HJ (2003) Homodimeric galectin-7 (p53-induced gene 1) is a negative growth regulator for human neuroblastoma cells. Oncogene 22:6277–6288

Kriz W, Bankir L (1988) A standard nomenclature for structures of the kidney. The Renal Commission of the International Union of Physiological Sciences (IUPS). Kidney Int 33:1–7

Langner C, Ratschek M, Rehak P, Schips L, Zigeuner R (2004) Steroid hormone receptor expression in renal cell carcinoma: an immunohistochemical analysis of 182 tumors. J Urol 171:604–611

Laurent G, Nonclercq D, Journé F, Brohée R, Toubeau G, Falmagne P, Heuson-Stiennon JA (1999) Characterization of a cell line established from diethylstilbestrol-induced renal tumors in Syrian hamsters. In Vitro Cell Dev Biol—Anim 35:339–344

Li JJ, Li SA (1984) Estrogen-induced tumorigenesis in hamsters: roles for hormonal and carcinogenic activities. Arch Toxicol 55:108–110

Li JJ, Li SA (1990) Estrogen carcinogenesis in hamster tissues: a critical review. Endocr Rev 11:524–531

Li JJ, Hou X, Banerjee SK, Liao DJ, Maggouta F, Norris JS, Li SA (1999) Overexpression and amplification of c-myc in the Syrian hamster kidney during estrogen carcinogenesis: a probable critical role in neoplastic transformation. Cancer Res 59:2340–2346

Li JJ, Weroha SJ, Davis MF, Tawfik O, Hou X, Li SA (2001) ER and PR in renomedullary interstitial cells during Syrian hamster estrogen-induced tumorigenesis: evidence for receptor-mediated oncogenesis. Endocrinology 142:4006–4014

Liehr JG (1997) Hormone-associated cancer: mechanistic similarities between human breast cancer and estrogen-induced kidney carcinogenesis in hamsters. Environ Health Perspect 105:565–569

Liehr JG (2001) Genotoxicity of the steroidal oestrogens oestrone and oestradiol: possible mechanism of uterine and mammary cancer development. Hum Reprod Update 7:273–281

Liehr JG, Fang WF, Sirbasku DA, Ari-Ulubelen A (1986) Carcinogenicity of catechol estrogens in Syrian hamsters. J Steroid Biochem 24:353–356

Lindblad P, Mellemgaard A, Schlehofer B, Adami HO, McCredie M, McLaughlin JK, Mandel JS (1995) International renal-cell cancer study. V. Reproductive factors, gynecologic operations and exogenous hormones. Int J Cancer 61:192–198

Liu FT, Patterson RJ, Wang JL (2002) Intracellular functions of galectins. Biochim Biophys Acta 1572:263–273

López-Lucendo MF, Solís D, André S, Hirabayashi J, Kasai KI, Kaltner H, Gabius HJ, Romero A (2004) Growth-regulatory human galectin-1: crystallographic characterisation of the structural changes induced by single-site mutations and their impact on the thermodynamics of ligand binding. J Mol Biol 343:957–970

Manning JC, Seyrek K, Kaltner H, André S, Sinowatz F, Gabius HJ (2004) Glycomic profiling of developmental changes in bovine testis by lectin histochemistry and further analysis of the most prominent alteration on the level of the glycoproteome by lectin blotting and lectin affinity chromatography. Histol Histopathol 19:1043–1060

Morris S, Ahmad N, André S, Kaltner H, Gabius HJ, Brenowitz M, Brewer F (2004) Quaternary solution structures of galectins-1, -3, and -7. Glycobiology 14:293–300

Nagy N, Bronckart Y, Camby I, Legendre H, Lahm H, Kaltner H, Hadari Y, Van Ham P, Yeaton P, Pector JC, Zick Y, Salmon I, Danguy A, Kiss R, Gabius HJ (2002) Galectin-8 expression decreases in cancer as compared to normal and dysplastic human colon tissue and acts significantly on human colon cancer cell migration. Gut 50:392–401

Nagy N, Legendre H, Engels O, André S, Kaltner H, Wasano K, Zick Y, Pector JC, Decaestecker C, Gabius HJ, Salmon I, Kiss R (2003) Refined prognostic evaluation in colon carcinoma using immunohistochemical galectin fingerprinting. Cancer 97:1849–1858

Nogueira E, Gardesa A, Mohr U (1993) Experimental models of kidney tumors. J Cancer Res Clin Oncol 119:190–198

Nonclercq D, Toubeau G, Wattiez R, LaurentG, Bernard A, Journe F, Falmagne P, Heuson-Stiennon JA (1998) Sublethal alterations and sustained cell proliferation associated with diethylstilbestrol-induced renal carcinogenesis in male Syrian golden hamsters. Eur J Morphol 36:83–96

Nonclercq D, Lienard V, Zanen J, Laurent G, Toubeau G (2002) Phenotypic variation and dynamic topography of transformed cells in an experimental model of diethylstilbestrol-induced renal tumor in male Syrian hamster. Histochem J 34:487–497

Orovan WL, Ryan ED (1989) Estrogen and progesterone binding sites in renal cell carcinoma. Urology 34:65–67

Paron I, Scaloni A, Pines A, Bachi A, Liu FT, Puppin C, Pandolfi M, Ledda L, Di Loreto C, Damante G, Tell G (2003) Nuclear localization of galectin-3 in transformed thyroid cells: a role in transcriptional regulation. Biochem Biophys Res Commun 302:545–553

Purkrábková T, Smetana K Jr, Dvoránková B, Holíková Z, Böck C, Lensch M, André S, Pytlík R, Liu FT, Klíma J, Smetana K, Motlík J, Gabius HJ (2003) New aspects of galectin functionality in nuclei of cultured bone marrow stromal and epidermal cells: biotinylated galectins as tool to detect specific binding sites. Biol Cell 95:535–545

Rappl G, Abken H, Muche JM, Sterry W, Tilgen W, André S, Kaltner H, Ugurel S, Gabius HJ, Reinhold U (2002) CD4+CD7− leukemic T cells from patients with Sézary syndrome are protected from galectin-1-triggered T cell death. Leukemia 16:840–845

Rotblat B, Niv H, André S, Kaltner H, Gabius HJ, Kloog Y (2004) Galectin-1(L11A) predicted from a computed galectin-1 farnesyl-binding pocket selectively inhibits Ras-GTP. Cancer Res 64:3112–3118

Sanford GL, Owens MA, Odusanya BM (1993) Differential influence of dexamethasone on the activity and synthesis of β-galactoside specific lectin (galaptin) during postnatal lung development. Exp Lung Res 19:91–104

Saussez S, Nonclercq D, Laurent G, Wattiez R, André S, Kaltner H, Gabius HJ, Kiss R, Toubeau G (2005) Toward functional glycomics by localization of tissue lectins: immunohistochemical galectin fingerprinting during diethylstilbestrol-induced kidney tumorigenesis in male Syrian hamster. Histochem Cell Biol 123:29–41

Shimura T, Takenaka Y, Tsutsumi S, Hogan V, Kikuchi A, Raz A (2004) Galectin-3, a novel binding partner of β-catenin. Cancer Res 64:6363–6367

Siebert HC, André S, Lu SY, Frank M, Kaltner H, van Kuik JA, Korchagina EY, Bovin NV, Tajkhorshid E, Kaptein R, Vliegenthart JFG, von der Lieth CW, Jiménez-Barbero J, Kopitz J, Gabius HJ (2003) Unique conformer selection of human growth-regulatory lectin galectin-1 for ganglioside GM_1 versus bacterial toxins. Biochemistry 42:14762–14773

Spicer SS, Schulte BA (1992) Diversity of cell glycoconjugates shown histochemically: a perspective. J Histochem Cytochem 40:1–38

Toubeau G, Nonclercq D, Laurent G, Brohee R, Zanen J, Van Cauwenberge A, Alexandre H, Falmagne P, Heuson-Stiennon JA (2001) Immunohistochemical analysis of diethylstilbestrol-induced renal tumors in adult male Syrian hamsters: evidence for relationship to peripheral nerve sheath tumors. Histochem Cell Biol 115:429–438

Unverzagt C, André S, Seifert J, Kojima S, Fink C, Srikrishna G, Freeze H, Kayser K, Gabius HJ (2002) Structure–activity profiles of complex biantennary glycans with core fucosylation and with/without additional α2,3/α2,6 sialylation: synthesis of neoglycoproteins and their properties in lectin assays, cell binding, and organ uptake. J Med Chem 45:478–491

Villalobo AV, Nogales-Gonzalez A, Gabius HJ (2006) A guide to signalling pathways connecting protein–glycan interaction with the emerging versatile effector functionality of mammalian lectins. Trends Glycosci Glycotechnol (in press)

Wada T, Nishiyama K, Maeda M, Hara S, Tanaka N, Yasutomi M, Kurita T (1995) Combined chemoendocrine treatment with tegafur and tamoxifen for advanced renal cell carcinoma. Anticancer Res 15:1581–1584

Wattiez R, Nonclercq D, Journe F, Toubeau G, Zanen J, Falmagne P, Heuson-Stiennon JA (1996) Involvement of transforming growth factor α and its receptor in a model of DES-induced renal carcinogenesis in the Syrian hamster. Carcinogenesis 17:1615–1622

Winyard PJ, Bao Q, Hughes RC, Woolf AS (1997) Epithelial galectin-3 during human nephrogenesis and childhood cystic diseases. J Am Soc Nephrol 8:1647–1657

Wu AM, Wu JH, Liu JH, Singh T, André S, Kaltner H, Gabius HJ (2004) Effects of polyvalency of glycotopes and natural modifications of human blood group ABH/Lewis sugars at

the Galβ1-terminated core saccharides on the binding of domain-I of recombinant tandem-repeat-type galectin-4 from rat gastrointestinal tract (G4-N). Biochimie 86:317–326

Young AN, Amin MB, Moreno CS, Lim SD, Cohen C, Petros JA, Marshall FF, Neish AS (2001) Expression profiling of renal epithelial neoplasms: a method for tumor classification and discovery of diagnostic molecular markers. Am J Pathol 158:1639–1651